J Fluoresc (2007) 17:163–170
DOI 10.1007/s10895-006-0154-0

ORIGINAL PAPER

Rotational Relaxation of Linear π-Systems with Flexible Side Chains in Solution

Ulrich-W. Grummt · Eckhard Birckner · Reinhold Gade

Received: 29 September 2006 / Accepted: 4 December 2006 / Published online: 1 February 2007

Abstract The classical hydrodynamic theory for Brownian rotational motion is applied to model compounds of conjugated polymers with alkoxy side chains of variable length. Theory predicts two rotational relaxation times for these types of molecules with the dipole transition moment parallel to the longest axis whereas experiments reveal only one. The rotational relaxation times and their relative amplitudes were calculated for a wide span of axial ratios of a general ellipsoid. In this way, the range in the axial ratios is obtained such that there is a chance to detect both rates experimentally. Rotational relaxation times of five particular molecules were measured in liquid n-butane. Theoretical calculations using ellipsoid parameters obtained from molecular dynamics calculations compare well with experimental results. Calculation of the rotational relaxation times from the autocorrelation function of the transition dipole moment vector requires significantly greater computational effort.

Keywords Molecular dynamics · Emission anisotropy · Conjugated polymers · Fluorescence · Energy migration

Introduction

The prediction of the stationary emission anisotropy, r_{stat}, of rigid spherical molecules from their rotational relaxation times, ρ, and their fluorescence lifetimes, τ, with the help of the Perrin equation [1] is among the standard tools of photophysics [2].

$$r_{\mathrm{stat}} = \frac{r_0}{1 + \frac{\tau}{\rho}} \tag{1}$$

The limiting anisotropy for randomly oriented fluorophores is given by

$$r_0 = \frac{3\ \cos^2\ \alpha - 1}{5} \tag{2}$$

where α is the angle between the transition moments for absorption and emission.
The rotational relaxation time, ρ, can be obtained from the Stokes-Einstein relation where V_{rot} is the rotational volume and η is the solvent viscosity:

$$\rho = \frac{\eta V_{\mathrm{rot}}}{kT} \tag{3}$$

The theory also generalizes well to certain cases involving non spherical molecules [3]. In the case of symmetric tops, there is still only one rotational relaxation time as long as the transition moments are parallel to the top axis. We have recently proposed a significant simplification for the prediction of rotational relaxation times for symmetric tops of the prolate type [4] for an axial ratio $1 < a/b < 8$, where a and b are the long and short half-axes of the top, respectively, the rotational volume can be approximated well by

$$V_{\mathrm{rot}} = \frac{4\pi}{3} a^2 b \tag{4}$$

In the case of asymmetric tops, theory allows up to five different rotational relaxation times [5]. However, to the best of

U.-W. Grummt (✉) · E. Birckner · R. Gade
Institut für Physikalische Chemie,
Friedrich-Schiller-Universität Jena,
Helmholtzweg 4,
D-07743 Jena, Germany
e-mail: cug@uni-jena.de

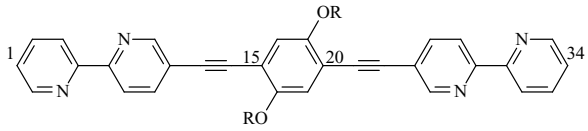

Scheme 1 Molecular structures and abbreviations of the model compounds investigated; R = *n*-butyl (**Bu**), R = *n*-octyl (**Oc**), R = 2-ethyl-hexyl (**EH**), R = *n*-dodecyl (**Dd**), and R = *n*-octadecyl (**Od**)

our knowledge it is not yet possible to resolve the kinetics to such a level. Isenberg and Small [6] have shown that there are relationships between the time constants. According to these authors, at most only three exponentials will be observable. Of these, only two are independent.

In the present paper we investigate fluorescent molecules which bear long flexible side chains, the structures of which are shown in Scheme 1. These molecules are model compounds for conjugated poly(hetero-arylene-ethynylene)s. Abbreviations of the alkyl substituents will be used as substance codes. The π-system responsible for absorption and emission may still be approximated as a prolate symmetrical top, although dynamic distortions of the ideal linear chromophores are allowed.

The side chains render these molecules asymmetric tops. The first objective of this paper is to determine whether the experimentally observed smooth first order decay of the fluorescence anisotropy is consistent with the known theory which is briefly outlined here.

If a, b, and c are the half-axes of an ellipsoid, then the principal friction coefficients C_i can be obtained according to Perrin [7] and Edwardes [8] from the following equations

$$C_1 = \frac{160\pi}{3}\eta\frac{b^2+c^2}{b^2Q+c^2R} \quad C_2 = \frac{160\pi}{3}\eta\frac{a^2+c^2}{a^2P+c^2R} \quad C_3 = \frac{160\pi}{3}\eta\frac{a^2+b^2}{a^2P+b^2Q} \tag{5}$$

where η is the dynamic viscosity of the solvent in Pas. The elliptic integrals

$$P = \int_0^\infty \frac{ds}{(a^2+s)\sqrt{(a^2+s)(b^2+s)(c^2+s)}} \tag{6}$$

$$Q = \int_0^\infty \frac{ds}{(b^2+s)\sqrt{(a^2+s)(b^2+s)(c^2+s)}} \tag{7}$$

$$R = \int_0^\infty \frac{ds}{(c^2+s)\sqrt{(a^2+s)(b^2+s)(c^2+s)}} \tag{8}$$

are related by the equations

$$P+Q+R = \frac{2}{abc} \quad \text{and} \quad a^2P+b^2Q+c^2R = S \tag{9}$$

where S is given by

$$S = \int_0^\infty \frac{ds}{\sqrt{(a^2+s)(b^2+s)(c^2+s)}} \tag{10}$$

The rotational diffusion coefficients are simple functions of the friction coefficients:

$$D_1 = \frac{kT}{C_1} \quad D_2 = \frac{kT}{C_2} \quad D_2 = \frac{kT}{C_3} \tag{11}$$

In Perrin's notation the rotational diffusion coefficients differ by a factor of 4 from the values given above, cf. Memming's paper [9]. These approximations are valid for stick conditions if the rotational motions are slow.

The relations between the rotational diffusion coefficients and the rotational relaxation times have been given by Tao [5]. The appropriate equations specified for the type of molecules under investigation will be given below.

The second purpose of this paper is to show that molecular dynamics calculations can deliver effective mean rotational volumes which, in turn, can be used to predict time-dependent and stationary emission anisotropies. In principle, the time-dependent fluorescent anisotropy $r(t)$ can also be obtained from the autocorrelation function of the transition moment vectors

$$r(t) = r_0\langle P_2(\mu(0)\cdot\mu(t))\rangle \tag{12}$$

where P_2 is the Legendre polynomial of order 2. The general formulation of the autocorrelation function

$$R(\tau) = \lim_{T\Rightarrow\infty}\frac{1}{T}\int_{t=\tau}^{T} y(t)y(t-\tau)\,dt \tag{13}$$

must be recast in discrete form to be practically applicable:

$$R_j = \frac{\Delta T}{T}\sum_{i=j}^{n} y_i y_{i-j} = \frac{1}{n-j}\sum_{i=j}^{n} y_i y_{i-j} \tag{14}$$

We want to determine which one of these two alternatives, the calculation either from the molecular shape with the help of the hydrodynamic theory or from the autocorrelation function, is more appropriate.

Finally, we want to show that mean angles formed by chromophore units on a conjugated polymer chain obtained from a molecular dynamics calculation can be used in connection

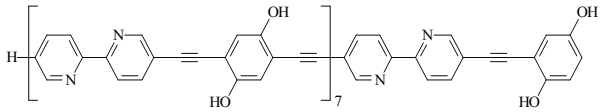

Scheme 2 Model oligomer called an 'octamer' for simplicity

with anisotropy measurements to determine the mean distance of energy migration along the polymer backbone. The type of polymer is depicted in Scheme 2.

The octamer is a hypothetical compound. Polymers of an analogous structure with alkoxy side chains instead of OH groups are described in reference [10].

Experimental and methods

The syntheses of compounds **1** to **5** are described in previous papers [11]. Stationary fluorescence measurements were performed in liquid butane at room temperature with the help of an LS50B spectrofluorometer (Perkin Elmer). Fluorescence kinetics and anisotropy kinetics were recorded with a single photon counting spectrometer equipped with an MCP-PMT R3809U-50 (Hamamatsu) and an SPC430 card (Becker & Hickl, Berlin). The channel width was 6 ps. The overall response time of the system is 85 ps without deconvolution, cf. the instrument response function shown in Fig. 2. A picosecond laser diode emitting at 405 nm (Picoquant, Berlin) was used as an excitation source. Glan-Thompson prisms were used as the polarizer and analyzer.

The solvent *n*-butane was purchased from Air-Liquide as 99.999% pure product. It was stored for at least one day over charcoal in a steel cylinder because it showed significant fluorescence as delivered. Ordinary 1 cm × 1 cm fused quartz cells with tight-fitting stopcocks were used for the spectroscopic measurements. A well defined small amount of chloroform solution of the appropriate concentration to yield a final absorbance $0.3 < A < 0.4$ at the excitation wavelength was first filled into the cells. The solvent was allowed to evaporate. Then the cell was filled directly with butane at atmospheric pressure and room temperature through a thin stainless steel pipe. Due to the heat consumption of the evaporating butane, a sufficient amount of butane condensed rapidly to fill the cell. With thoroughly fixed stopcocks, the sample could be stored under ambient conditions for more than a week without an appreciable loss of solvent.

The LEVEL 2 (Edinburgh Analytical Instruments), spherical rotor kinetics was applied for the evaluation of the experimental anisotropy decay traces. Briefly, this kinetic model performs a simultaneous Marquardt fit of both the crossed and the parallel data files of an anisotropy measurement (subscript $\perp$ and $||$, respectively). The fits produced are of the form

$$Y_\perp = A_\perp + B_\perp[1 - r_0 e^{-t/\rho}]e^{-t/\tau} \tag{15a}$$

$$Y_{||} = A_{||} + B_{||}[1 + 2r_0 e^{-t/\rho}]e^{-t/\tau}. \tag{15a}$$

The TINKER program [12] was used for the molecular dynamics calculations in connection with Allinger's MM3 force field. No special assumptions were made with respect to solvent-solvent and solute-solvent interactions other than the validity of the Lennard-Jones potential describing the van der Waals interactions. The time step chosen was 0.5 fs. All dynamics calculations were extended to a total time of (at least) 1 ns if not otherwise stated. Snapshots were archived every 0.5 ps, such that 2000 snapshots were evaluated for each sample.

After the solute molecules were removed from the solvent box, they were rotated to the coordinate system of their principal axes of inertia. The maximal distances between two atoms along these axes were taken as the diameters of the rotational ellipsoid.

The solvent box dimensions chosen were $4.0 \times 4.0 \times 4$ nm with the exception of **Od** which required a box of $6.0 \times 4.0 \times 4.0$ nm. The number of butane molecules in the boxes was adjusted to generate a density of $0.59 < \delta < 0.60\ \mathrm{kg\ m^{-3}}$, which is the density at the boiling point. The viscosity $\eta = 156\ \mu$Pas was taken from reference [13] by linear extrapolation of the pressure-dependent data given for 300 K to a pressure of 2 bar. The canonical ensemble was chosen for the simulations of the periodic systems.

Results and discussion

With the dipole transition moment parallel to the longest principal axis of momentum, the rather involved equations derived by Tao simplify considerably. Only two of a maximum of five relaxation times survive which leads to an anisotropy decay given by

$$r(t) = \frac{2}{5}P_2(\cos\varphi)\left[\left(\frac{1}{2} + \frac{2D_1 - D_2 - D_3}{4\Delta}\right)e^{-(6D-2\Delta)t} + \left(\frac{1}{2} - \frac{2D_1 - D_2 - D_3}{4\Delta}\right)e^{-(6D+2\Delta)t}\right] \tag{16}$$

with

$$D = \frac{D_1 + D_2 + D_3}{3}$$

and

$$\Delta = \sqrt{D_1^2 + D_2^2 + D_3^2 - D_1D_2 - D_1D_3 - D_2D_3}$$

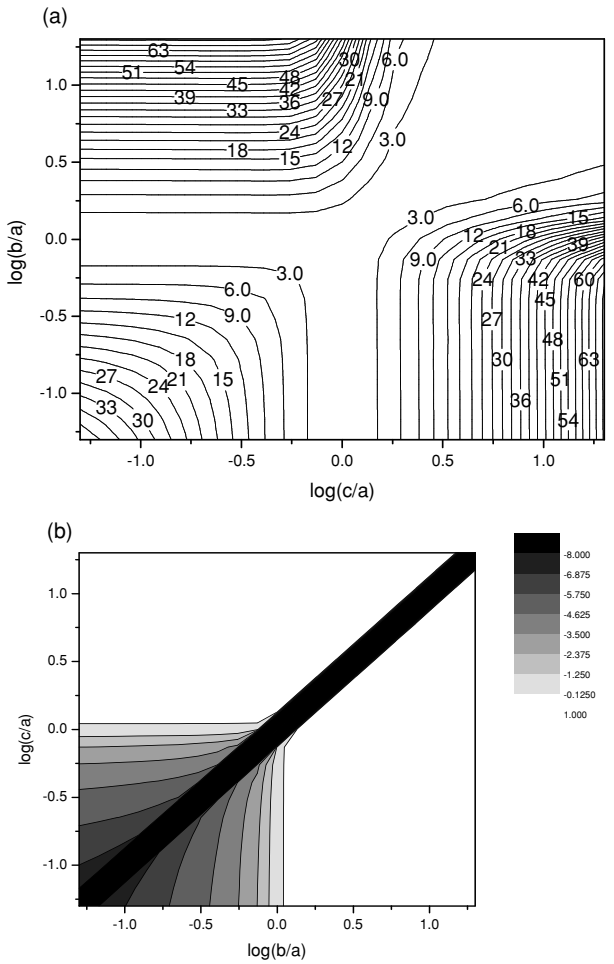

Fig. 1 a. Contour plot of the ratio ρ_1/ρ_2 as a function of the axial ratios b/a and c/a (logarithmic scales). b. Contour plot of $\log(a_2/a_1)$ as a function of the axial ratios $\log(b/a)$ and $\log(c/a)$

and $P_2(\cos\varphi) = \frac{3\cos^2\varphi - 1}{2}$, the Legendre polynomial of order 2.

We have solved the above equations for a grid of axial ratios

$$\frac{1}{20} \le \frac{b}{a} \le 20 \quad \text{and} \quad \frac{1}{20} \le \frac{c}{a} \le 20. \tag{17}$$

The numerical results are shown in Fig. 1a and b, where the ratio ρ_2/ρ_1 and the logarithm of the amplitude ratio a_2/a_1 are plotted against the logarithms of the axial ratios. It is obvious from this general result that there is a real chance of detecting biexponential anisotropy decay only in the overlap regions of the contour lines $\rho_2/\rho_1 > 3$ as shown in the white area of Fig. 1b.

In the case of the particular molecules under study, the mean lengths of the principal axes were determined in the following way. At least 1000 snapshots from a dynamics run were stored and the molecules were rotated to the coordinate system of the principal axes of inertia. The largest distances along these axes were averaged to yield an estimate of the lengths. The longest axis coincides with the extension of the π-system for all compounds except **Od** The longest principal axis of **Od** is determined by the extension of the side chains. The second principal axis is the projection of the π-system on the normal of the first axis, yielding a mean angle of 55 degrees between the transition moment and the longest principal axis. The transition dipole component in the direction of the third principal axis vanishes, suggesting that three exponentials are expected to generate the anisotropy decay:

$$r(t) = r_0 \Big[(3\cos^2\varphi\,\sin^2\varphi) e^{-3(D_3+D)t} + \frac{3}{4}(B+A) e^{-(6D-2\Delta)t} + \frac{3}{4}(B-A) e^{-(6D+2\Delta)t} \Big]$$

with

$$A = \frac{1}{\Delta}(D_1\cos^4\varphi + D_2\sin^4\varphi + 2D_3\cos^2\varphi\,\sin^2\varphi - D)$$

and

$$B = \cos^4\varphi + \sin^4\varphi - \frac{1}{3} \tag{18}$$

Numerical evaluation of the above equations using the mean geometry data from the MD calculations results in three lifetimes of very similar magnitude (233, 249 and 179 ps). The amplitude of the second component is negligibly small. The remaining two exponentials are so close together that they cannot be separated with the given signal-to-noise ratio. The weighted mean is given in Table 1.

For the molecules under study, $a > b > c$ holds and the axial ratios vary in the narrow regions as obtained from the molecular dynamics calculations.

Table 2 shows the experimental data obtained in *n*-butane solvent at room temperature. One example of a polarized fluorescence decay measurement together with the fitted curves is given in Fig. 2. The instrument response function is also included.

Table 1 Ellipsoid diameters, rotational relaxation times and stationary anisotropies obtained from the molecular dynamics calculations

Compound	d_x/Å	d_y/Å	d_z/Å	ρ/ps	r_{stat}
Bu	26.6 ± 0.4	13.3 ± 1.5	5.4 ± 1.1	102	0.031
Oc	26.5 ± 0.5	15.4 ± 1.5	7.6 ± 1.0	133	0.039
EH	26.1 ± 0.6	16.9 ± 4.2	6.7 ± 1.4	129	0.038
Dd	27.3 ± 3.2	21.5 ± 3.1	8.8 ± 2.0	160	0.045
Od	31.9 ± 3.8	21.8 ± 2.6	11.5 ± 2.3	215	0.059

Table 2 Fluorescence lifetimes and experimental anisotropy data obtained in *n*-butane solvent at room temperature

Compound	τ/ns	ρ/ps	r_0	r_{kin} [a]	r_{stat} [b]
Bu	1.220 ± 0.003	85	0.369	0.0277	0.022 ± 0.005
Oc	1.245 ± 0.010	94.5 ± 2.7	0.373 ± 0.001	0.0307 ± 0.0004	0.028 ± 0.010
EH	1.245 ± 0.003	96.9 ± 1.8	0.370 ± 0.004	0.0312 ± 0.0003	0.0263 ± 0.004
Dd	1.257 ± 0.001	109.0 ± 2.3	0.362 ± 0.004	0.0344 ± 0.0002	0.0287 ± 0.0084
Od	1.235 ± 0.007	134.4 ± 2.5	0.355 ± 0.006	0.0434 ± 0.0001	0.031 ± 0.0035

[a] $r_{kin} = r_0/(1 + \tau/\rho)$.
[b] $r_{stat} = (I_{VV} - G\,I_{VH})/(I_{VV} - 2G\,I_{VH})$; $G = I_{HV}/I_{HH}$.

These data are to be compared with theoretical values obtained from the molecular dynamics calculations shown in Table 1. If we take into account the rather crude approximation of the irregular molecular shapes being represented as ellipsoids and the simplifications made in the derivation of the theory, then the deviations between the experimental and calculated rotational relaxation times are surprisingly small. Remarkably, the difference between the predicted and the experimental relaxation times increases systematically with increasing length of the side chains. This means that the outermost segments of the side chains become less involved in rotational diffusion of the π-systems as the side chains become longer.

As an alternative method, we have calculated a series of anisotropy decay curves from the autocorrelation function as described above. An example is shown in Fig. 3a. The simulated anisotropy decay curves are normalized to a starting value of $r_0 = 0.4$. Figure 3b shows an exponential fit of the weighted and averaged decay curves. It is obvious from Fig. 3, that a single dynamics run over about three rotational relaxation times is by far insufficient to obtain a reasonable anisotropy decay curve, whereas averaging the molecular shape over the same time interval already yields representative lengths of the axes. At least one order of magnitude larger computational effort is required to obtain reliable rotational relaxation times via the autocorrelation function from molecular dynamics. Hence we conclude that the prediction of anisotropy decay rates via calculation of the rotational volume is more efficient, at least for the types of molecules investigated in this study.

As pointed out by Wegener et al. [14] a long rigid rod bent at its center, as an example, cannot always be represented by an equivalent ellipsoid. The elongated molecules studied in this work, if bent due to thermal excitation, might belong to this class. The bending vibrations are in the order of magnitude of 10 cm^{-1} [15] which means, that this bending is leveled off within a few picoseconds.

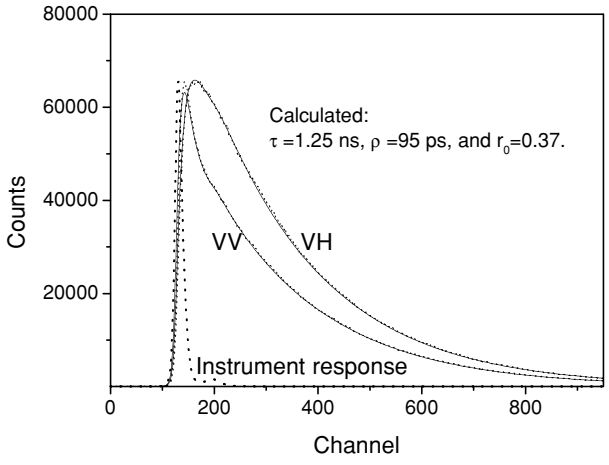

Fig. 2 Experimental and fitted VV (vertical/vertical) and VH (vertical/horizontal) components of the fluorescence decay of **Oc** in liquid butane at room temperature, and the intrument response function

Energy migration along the polymer chain

In a conjugated polymer the excitation energy is localized to finite chain sections even if the π-system is perfectly flat. Energy migration along a rigid and perfectly linear conjugated polymer chain does not change the direction of the emission dipole moment and will not contribute to fluorescence depolarization. If the polymer chain is bent, then energy migration leads to a decrease of the fluorescence anisotropy (Scheme 3). If the average transfer occurs from chromophore1 to chromophore i, then the stationary emission anisotropy can be calculated as

$$r_{1i} = \frac{3\langle\cos^2\varphi_{1i}\rangle - 1}{5} \tag{19}$$

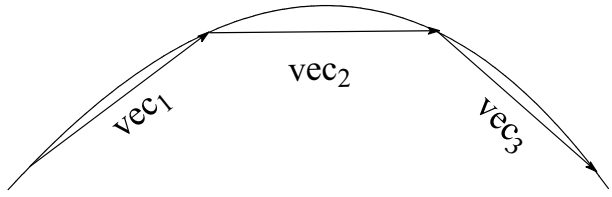

Scheme 3 The vectors vec_i symbolize the dipole transition moments of adjacent spectroscopic units along a bent polymer nbackbone

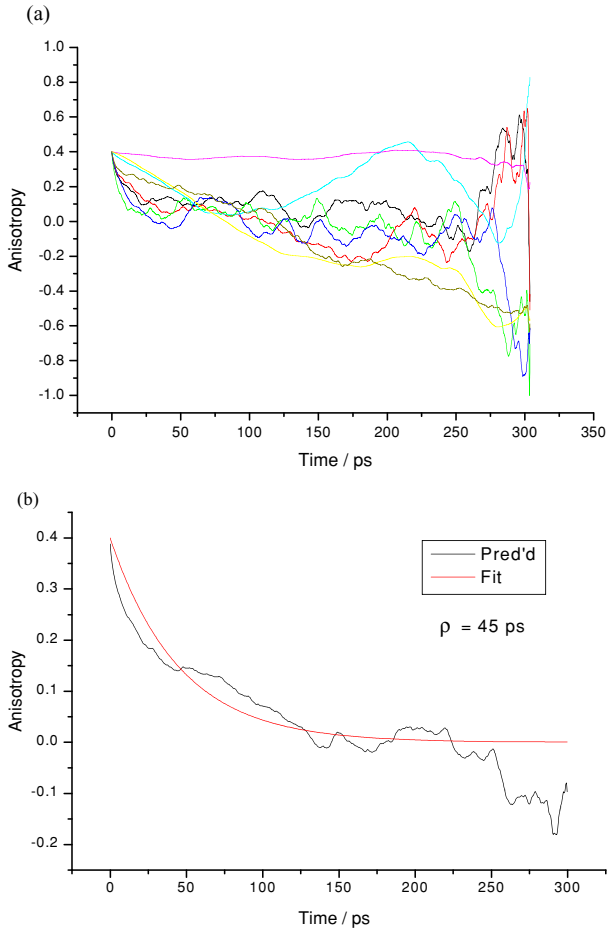

Fig. 3 a. Fluorescence anisotropy decay curves from MD simulations. b. Averaged anisotropy decay curves from Fig. 3a and exponential fit; $r_0 = 0.4$ was kept constant. Data points were weighted proportional to $n - j$ in Eq. (14). (Note that this anisotropy decay is not weighted by the fluorescence intensity decay)

where

$$\varphi_{1i} = \arccos \frac{vec_1\, vec_i}{|vec_1||vec_i|}$$

MD simulations with **Om** were performed in the gas phase in order to keep the computational effort affordable. A series of simulations with **EH** was first performed in the gas phase at various temperatures. The mean bending angle between the vectors defined by the pairs of atoms 1, 15 and 20, 34 in Scheme 1 was the same for the molecule in the solvent box at 300 K and in the gas phase at 250 K. Hence, this temperature was chosen for all gas phase simulations.

Polymers of the same structural type as **Om** show an effective conjugation length of about two repetition units at room temperature [10]. Thus, we defined the directions of the transition moment vectors by two terminal C-atoms of two consecutive repetition units. We determined the mean angle between adjacent transition moments for all possible pairs on the chain from a total of 8 independent MD runs, which resulted in an anisotropy of $r_{stat} = 0.1 \pm 0.1$. This means that if energy transfer quantitatively proceeded to the nearest spectroscopic unit, then the stationary emission anisotropy should already vanish completely. Since the experimental anisotropy of the polymer is $0.2 < r_{stat} < 0.3$ [10], we must conclude from the molecular dynamics results that energy transfer along the polymer backbone is inefficient. This result is in accord with recent quenching experiments [10].

Occasionally the fluorescence anisotropy increased again to a value close to 0.4 for larger migration distances. Inspection of the geometry showed that loops had formed which remained relatively stable during the simulation time. Direct energy transfer to rather distant segments via loops has been reported by Barbara [16] with poly (*para*-phenylene vinylene) (PPV). This has hitherto not been observed with conjugated polymers of the poly (*para*-phenylene ethynylene) (PPE) type and may be a challenge for single molecule spectroscopy.

Segmental mobility also contributes to the stationary anisotropy and to the anisotropy decay, however, to a minor extent. Analogue analysis of appropriate autocorrelation functions gave rotational relaxation times with large uncertainties between 500 ps and 4 ns.

Conclusions

There exists a chance to experimentally observe two distinct rotational relaxation times with a completely asymmetric body approximated as an ellipsoid with the transition moments of absorption and emission collinear with the longest principal axis only if the following conditions are simultaneously fulfilled:

(i) The axial ratios must be $c/a > 1.1$ and $b/a < 0.9$ or vice versa. Otherwise the rates become too similar to be resolved, cf. Fig. 1a.
(ii) Both ratios b/a and c/a must be greater than 0.7. Otherwise one amplitude would become too small relative to the other one, cf. Fig. 1b.

It is assumed here that the signal-to-noise ratio will allow two rates to be resolved if $\rho_1 > 3\rho_2$ and $0.1 > a_1/a_2 < 10$.

A main finding of this work is that the classical hydrodynamic theory of Brownian rotational motion is able to satisfactorily predict the rotational relaxation times for irregularly shaped rigid rod molecules with highly flexible side chains in a low molecular weight solvent. For that purpose, molecular dynamics simulations in a suitable solvent deliver averaged molecular geometries from which the principal axes of inertia of a general ellipsoid are determined. Although this procedure makes use of many more approximations and simplifications than the more straightforward

calculation from the autocorrelation function of the transition moment, it is superior because it requires less computational effort.

Acknowledgments We thank J. Ponder for advising us with details of his TINKER package. Valuable discussions with K.-L. Oehme are gratefully acknowledged.

Appendix

In order to derive Eqs. (16) and (18), we reproduce the equations derived by Tao for the fluorescence anisotropy decay of a general ellipsoid here in its entirety:

$$r(t) = \frac{2}{5}P_2\cos(\lambda)\left[\frac{3\mu_1^2\mu_2^2}{\mu^4}e^{-3(D_3+D)t} + \frac{3\mu_1^2\mu_3^2}{\mu^4}e^{-3(D_2+D)t} + \frac{3\mu_2^2\mu_3^2}{\mu^4}e^{-3(D_1+D)t} + \frac{3}{4}(B+A)e^{-(6D-2\Delta)t} + \frac{3}{4}(B-A)e^{-(6D+2\Delta)t}\right]$$

where

$$D = \frac{1}{3}(D_1+D_2+D_3),$$

$$\Delta = \sqrt{D_1^2+D_2^2+D_3^2-D_1D_2-D_1D_3-D_2D_3},$$

and

$$\frac{2}{5}P_2\cos(\lambda) = r_0$$

$$A = \frac{D_1}{\Delta}\left(\frac{\mu_1^4+2\mu_2^2\mu_3^2}{\mu^4}\right) + \frac{D_2}{\Delta}\left(\frac{\mu_2^4+2\mu_1^2\mu_3^2}{\mu_4}\right) + \frac{D_3}{\Delta}\left(\frac{\mu_3^4+2\mu_1^2\mu_2^2}{\mu_4}\right) - \frac{D}{\Delta},$$

and

$$B = \left[\frac{(\mu_1^4+\mu_2^4+\mu_3^4)}{\mu^4}\right] - \frac{1}{3}.$$

λ is the angle between the absorption and emission transition dipoles. ($\lambda = 0$ for all cases considered here.) The Cartesian components of the transition dipole moment μ are

$$\mu_1 = \mu\,\sin\theta'\,\cos\varphi' \quad \mu_2 = \mu\,\sin\theta'\,\sin\varphi' \quad \mu_3 = \mu\,\cos\theta',$$

where θ' and φ' are the angles defining the orientation of the transition dipole moment in the body fixed Cartesian coordinates.

Obviously, if

$$\mu_1 = \mu \neq 0 \quad \text{and} \quad \mu_2 = \mu_3 = 0,$$

then the first three exponential terms vanish. Furthermore,

$$A = \frac{D_1 - D}{\Delta}, \quad \text{and} \quad B = \frac{2}{3},$$

from which Eq. (16) is obtained.

Analogously, if

$$\mu_1 \neq 0, \quad \mu_2 \neq 0, \quad \mu_1 \neq \mu_2, \quad \text{and} \quad \mu_3 = 0,$$

then

$$A = \frac{1}{\mu^4\Delta}\left(D_1\mu_1^4 + D_2\mu_2^4 + 2D_3\mu_1^2\mu_2^2\right) - \frac{D}{\Delta} \quad \text{and} \quad B = \frac{\mu_1^4+\mu_2^4}{\mu^4},$$

which yields

$$r(t) = r_0\left[\frac{3\mu_1^2\mu_2^2}{\mu^4}e^{-3(D_3+D)t} + \frac{3}{4}(B+A)e^{-(6D-2\Delta)t} + \frac{3}{4}(B-A)e^{-(6D+2\Delta)t}\right].$$

Inserting the above expressions for the Cartesian components of μ and taking into account that $\theta' = 0$ gives Eq. (18).

References

1. Perrin F (1929) Ann Phys Ser 10 10:169–275
2. Lakowicz JR (1999) Principles of fluorescence spectroscopy, 2nd edn. Kluwer Academic/Plenum Press, New York, pp 291–319
3. Fleming GR (1986) Chemical applications of ultrafast spectroscopy, international series of monographs on chemistry, vol 13. Oxford University Press, Clarendon Press, Oxford, New York, pp 124–133
4. Birckner E, Grummt U-W (2004) On the fluorescence depolarization and the calculation of rotational relaxation times of rigid rod molecules. J Fluoresc 14(3):249–253
5. Tao T (1969) Time-dependent fluorescence depolarization and Brownian rotational diffusion coefficients of macromolecules. Biopolymers 8(5):609–632
6. Small EW, Isenberg I (1977) Hydrodynamic properties of a rigid molecule: Rotational and linear diffusion and fluorescence anisotroipy. Biopolymers 16(9):1907–1928
7. (a) Perrin F (1934) Mouvement Brownien d'un Ellipsoide (I). Dispersion diélectrique pour des molécules ellipsoidales. J Phys Rad Ser VII 5(10):497–511; (b) Perrin F (1936) Mouvement Brownien d'un Ellipsoide (II). Rotation libre et dépolarisation des

fluorescenes. Translation et diffusion de molécules ellipsoidales. J Phys Rad Ser VII 7(1):1–11
8. Edwardes D (1893) Steady motion of a viscous liquid in which an ellipsoid is constrained to rotate about a principal axis. Quart J Pure Appl Math 26:70–78
9. Memming R (1961) Theorie der Fluoreszenzpolarisation. Z Phys Chem NF 28:168–189
10. Grummt U-W, Pautzsch Th, Birckner E, Sauerbrey H, Utterodt A, Neugebauer U, Klemm E (2004) Photophysics of poly{2,2′-bipyridine-5,5′-diylethynylene[2,5-di(2-ethylhexyl)oxy-1,4-phenylene]ethynylene}: a comparison with monomer and dimer model compounds. J Phys Org Chem 17(3):199–206
11. (a) Grummt U-W, Birckner E, Klemm E, Egbe DAM, Heise B (2000) Conjugated polymers with 2,2′bipyridine and diethinylenebenzene units: absorption and luminescence properties. J Phys Org Chem 13(2):112–126; (b) Pautzsch Th, Klemm E (2002) Ruthenium-Chelating Poly(heteroaryleneethynylene)s: Synthesis and properties. Macromolecules 35(5):1569–1575
12. Ponder JW (2001) TINKER software tools for molecular design,Version 3.9, available from http://dasher.wustl.edu/tinker
13. Diller DE, Van Poolen LJ (1985) Measurements of the viscosities of saturated and compressed liquid normal butane and isobutane. Int J Thermophys 6(1):43–62
14. Wegener WA, Koester VJ, Dowben RM (1979) A general ellipsoid cannot always serve as a model for the rotational diffusion properties of arbitrarily shaped rigid molecules. Proc Natl Acad Sci USA 76(12):6356–6360
15. Grummt U-W (2006) unpublished results
16. Barbara PF, Gesquiere AJ, Park S-J, Lee YJ (2005) Single-molecule spectroscopy of conjugated polymers. Acc Chem Res 38(7):602–610